

Narrative: detailed accounting of thermodynamic terms.

A rough accounting of the overall thermodynamics of actinonin binding provides a context in which to compare the magnitude of local changes in conformational entropy, ΔS_{conf} , as measured from the change in order parameters (ΔS^2), to the overall entropy change (ΔS_{bind}). The free energy and the enthalpy of binding were $-9.8 \pm 1.3 \text{ kcal mol}^{-1}$ and $-1.644 \pm 0.012 \text{ kcal mol}^{-1}$ respectively, as measured by isothermal titration calorimetry. Neglecting differences between the standard state (1 M) and those of the NMR experiments (1 mM), from Gibbs relation, $\Delta G_{\text{bind}} = \Delta H_{\text{bind}} - T\Delta S_{\text{bind}}$, the corresponding entropic contribution to the binding free energy ($T\Delta S_{\text{bind}}$) is $+8.4 \pm 1.3 \text{ kcal mol}^{-1}$ at 310 K. This value includes increases in system entropy due to changes in solvation as well as losses due to translational, rotational and conformational entropy. As discussed above, the structure-based estimate of the solvation entropy change was $+13.3 \text{ kcal mol}^{-1}$ at 310 K. The net contributions due to conformational entropy and losses of rotational and translational degrees of freedom are $-4.66 \text{ kcal mol}^{-1}$ ($T\Delta S_{\text{bind}} - T\Delta S_{\text{solv}} = T\Delta S_{\text{r/t}} + T\Delta S_{\text{conf}}$) with the conformational entropy change contribution from the NMR dynamics experiments ≈ -4.01 to $3.87 \text{ kcal mol}^{-1}$. Estimates of the contributions due to loss of rotational/translational entropy remain controversial, ranging from negligible to $-15.5 \text{ kcal mol}^{-1}$ at 310 K ($-50 \text{ cal mol}^{-1} \text{ K}^{-1}$) (1-4). Given the NMR measurements, the resulting balance for binding-induced losses in rotational/translational degrees of freedom must range from -0.65 to $-8.53 \text{ kcal mol}^{-1}$. The crystal structure of free EcPDF contains a water molecule in the active site, as the fourth metal ligand, which is later displaced by actinonin. The entropic penalty associated with this water displacement has been estimated to be on the range of $T\Delta S \sim 0$ to 2 kcal mol^{-1} (5).

In addition to the entropic costs of conformational restrictions in EcPDF are the changes in conformational entropy of actinonin upon binding to the protein. Like all small linear peptide-like molecules, actinonin is highly flexible when free in solution, but adopts a well-defined structure when bound to the protein. In addition, NMR spectra of the free ligand (1D, 2D COSY, TOCSY; (6)) reveal that the amide bond between the L-valyl and L-prolinol groups is in slow exchange between *cis* and *trans* conformations in solution ($\sim 4:1$ *trans/cis* at 298 K). In contrast, only the *trans* conformation is observed in the crystal structure of the EcPDF-actinonin complex (7). The entropic costs of reducing the conformational flexibility of a ligand can be very significant (8). While they are not probed by the spectroscopic methods employed here, we have attempted to estimate this entropic penalty on statistical thermodynamic grounds (see Figure 11 and Figure 12). However, the large uncertainties in the measured entropic parameters, together with uncertainties in estimation limit the validity of conclusions based on these values.

Table 1. Heat of ionization of buffers used in ITC experiments (9, 10).

Buffer	Heat of Ionization (kcal/mol)	$K_A (M^{-1})$	ΔH (cal/mol)
TRIS	-11.34	$9.02E6 \pm 1.2E6$	-1644 ± 12
HEPES	-4.87	$4.23E6 \pm 4.8E5$	-1444 ± 15
Cacodylic Acid	-0.71	$9.98E6 \pm 8.3E6$	-1204 ± 47

Table 2. Per-residue NMR-derived structural and thermodynamic parameters for free and actinonin-bound PDF147. (ΔS_{conf} values are obtained by subtracting the residual entropy of the complex-free; positive values indicate an increase in dynamics. Positive $\Delta\Delta G$ values are stabilizing, corresponding to slower H/D exchange in the complex.)

Residue	S^2 PDF +actinonin	S^2 PDF	ΔS_{conf} \pm $\delta\Delta S_{\text{conf}}$	$\Delta\Delta G_{\text{HD}}$ \pm $\delta\Delta\Delta G_{\text{HD}}$	ΔrDC \pm $\delta\Delta rDC$
1 ALA					
2 VAL					
3 LEU	0.8637	0.8765	-0.2061 \pm 0.4535	0.000 \pm 0.616	0.015 \pm 0.140
4 GLN					
5 VAL	0.9203	0.9278	-0.2007 \pm 0.4327	0.000 \pm 0.616	0.179 \pm 0.074
6 LEU	0.9876	0.989	0 \pm 0.4109		
7 HIS	0.9197	0.914	0.14 \pm 0.3811	0.000 \pm 0.616	0.133 \pm 0.199
8 ILE	0.9268	0.9647	-1.2446 \pm 0.3645	0.477 \pm 0.022	0.364 \pm 0.104
9 PRO					
10 ASP	0.6064	0.4878	0.6578 \pm 0.9285	0.000 \pm 0.616	-0.133 \pm 0.216
11 GLU	0.9123	0.9132	-0.02 \pm 0.6164		
12 ARG	0.9357	0.9052	0.794 \pm 0.4308	0.000 \pm 0.616	-0.127 \pm 0.124
13 LEU	0.8856	0.881	0.0811 \pm 0.3517	-0.506 \pm 0.319	-0.183 \pm 0.067
14 ARG	0.8885	0.8821	0.1146 \pm 0.3637	-0.252 \pm 0.017	-0.042 \pm 0.110
15 LYS	0.8815	0.8695	0.2002 \pm 0.3767	0.384 \pm 0.043	0.149 \pm 0.200
16 VAL	0.8075	0.8142	-0.0769 \pm 0.3488	0.000 \pm 0.616	0.391 \pm 0.072
17 ALA				0.198 \pm 0.043	0.002 \pm 0.083
18 LYS	0.8532	0.8426	0.1458 \pm 0.3569	-0.173 \pm 0.382	-0.123 \pm 0.272
19 PRO					
20 VAL	0.8377	0.8331	0.0593 \pm 0.4081		0.105 \pm 0.123
21 GLU	0.8846	0.9075	-0.4553 \pm 0.559	0.000 \pm 0.616	-0.079 \pm 0.150
22 GLU				2.073 \pm 0.586	-0.040 \pm 0.041
23 VAL				0.000 \pm 0.616	-0.008 \pm 0.167
24 ASN	0.6871	0.6899	-0.0204 \pm 0.4516	-0.415 \pm 0.347	0.101 \pm 0.073
25 ALA					
26 GLU	0.8505	0.8447	0.0805 \pm 0.3643	0.000 \pm 0.616	-0.060 \pm 0.048
27 ILE	0.8516	0.8768	-0.3902 \pm 0.3683	-0.323 \pm 0.017	
28 GLN	0.9044	0.8965	0.1631 \pm 0.3886	-0.547 \pm 0.050	-0.156 \pm 0.086
29 ARG	0.8859	0.8888	-0.0525 \pm 0.3602	-0.493 \pm 0.025	-0.169 \pm 0.099

Residue	S^2 PDF +actinonin	S^2 PDF	ΔS_{conf}	$\pm \delta \Delta S_{\text{conf}}$	$\Delta \Delta G_{\text{HD}}$	$\pm \delta \Delta \Delta G_{\text{HD}}$	ΔrDC	$\pm \delta \Delta rDC$	
30	ILE						-0.617	\pm 0.068	
31	VAL	0.8823	0.8902	-0.144	\pm 0.3486	0.000	\pm 0.616	-0.087	\pm 0.065
32	ASP								
33	ASP	0.9147	0.9417	-0.7758	\pm 0.392	0.000	\pm 0.616	0.032	\pm 0.075
34	MET	0.8873	0.8957	-0.1615	\pm 0.4112	0.000	\pm 0.616	-0.062	\pm 0.140
35	PHE	0.8869	0.8957	-0.167	\pm 0.3635	0.000	\pm 0.616	0.020	\pm 0.079
36	GLU	0.8776	0.9028	-0.4783	\pm 0.356	0.000	\pm 0.616	0.015	\pm 0.055
37	THR	0.8872	0.8955	-0.1574	\pm 0.3389	0.000	\pm 0.616	0.027	\pm 0.077
38	MET	0.8777	0.8865	-0.1562	\pm 0.3562	0.000	\pm 0.616	-0.006	\pm 0.136
39	TYR	0.8866	0.8955	-0.1695	\pm 0.3542	0.000	\pm 0.616	-0.028	\pm 0.087
40	ALA						0.585	\pm 0.061	
41	GLU	0.8597	0.8673	-0.1173	\pm 0.4279	0.682	\pm 0.063	0.178	\pm 0.078
42	GLU	0.8394	0.8349	0.0587	\pm 0.3584	0.000	\pm 0.616	-0.007	\pm 0.085
43	GLY					1.482	\pm 0.093	-0.082	\pm 0.103
44	ILE								
45	GLY	0.9165	0.8964	0.4436	\pm 0.4229	2.186	\pm 0.368	-0.190	\pm 0.078
46	LEU					0.000	\pm 0.616	0.722	\pm 0.101
47	ALA	0.9079	0.8776	0.5898	\pm 0.4187	2.584	\pm 0.559	-0.324	\pm 0.147
48	ALA					0.000	\pm 0.616	-0.092	\pm 0.084
49	THR	0.9221	0.9419	-0.5966	\pm 0.3616	0.450	\pm 0.014	-0.178	\pm 0.060
50	GLN	0.8809	0.9137	-0.666	\pm 0.3553	0.000	\pm 0.616	0.173	\pm 0.081
51	VAL	0.9007	0.8903	0.2051	\pm 0.3828	0.000	\pm 0.616	-0.112	\pm 0.096
52	ASP						0.409	\pm 0.122	
53	ILE	0.8952	0.8222	1.1094	\pm 0.4043	0.000	\pm 0.616	0.060	\pm 0.066
54	HIS						-0.126	\pm 0.238	
55	GLN					1.817	\pm 0.365	-0.322	\pm 0.104
56	ARG								
57	ILE	0.8373	0.8514	-0.1913	\pm 0.4293	0.000	\pm 0.616	-0.001	\pm 0.080
58	ILE					0.000	\pm 0.616	-0.070	\pm 0.095
59	VAL	0.8909	0.8952	-0.0823	\pm 0.3486	0.000	\pm 0.616	0.088	\pm 0.091
60	ILE	0.8429	0.8367	0.0818	\pm 0.3575	0.000	\pm 0.616	-0.040	\pm 0.078
61	ASP	0.8483	0.8622	-0.2022	\pm 0.3689	0.000	\pm 0.616	0.184	\pm 0.072
62	VAL	0.8408	0.8539	-0.1807	\pm 0.3772	-0.314	\pm 0.025	-0.160	\pm 0.103
63	SER	0.9045	0.8868	0.3518	\pm 0.3947	-0.050	\pm 0.552	0.016	\pm 0.092
64	GLU					0.000	\pm 0.616	-0.064	\pm 0.079
65	ASN	0.8603	0.8473	0.1876	\pm 0.3788	0.000	\pm 0.616	-0.188	\pm 0.072
66	ARG	0.8933	0.8842	0.1679	\pm 0.3812	0.000	\pm 0.616	0.073	\pm 0.102
67	ASP	0.8525	0.8438	0.1208	\pm 0.3825	0.000	\pm 0.616	-0.121	\pm 0.066
68	GLU								
69	ARG	0.7369	0.8684	-1.488	\pm 0.3675			0.816	\pm 0.073
70	LEU					0.000	\pm 0.616	-0.113	\pm 0.104
71	VAL							0.518	\pm 0.071

Residue		S ² PDF +actinonin	S ² PDF	ΔS_{conf} \pm $\delta \Delta S_{\text{conf}}$	$\Delta \Delta G_{\text{HD}}$ \pm $\delta \Delta \Delta G_{\text{HD}}$	ΔrDC \pm $\delta \Delta rDC$
72	LEU	0.8637	0.8647	-0.0161 \pm 0.3808	0.000 \pm 0.616	-0.111 \pm 0.087
73	ILE	0.84	0.8343	0.0746 \pm 0.4065	0.000 \pm 0.616	0.179 \pm 0.097
74	ASN	0.8982	0.8777	0.3813 \pm 0.3649	0.000 \pm 0.616	-0.065 \pm 0.117
75	PRO					
76	GLU	0.8428	0.8301	0.1644 \pm 0.3488	-1.841 \pm 0.550	0.200 \pm 0.093
77	LEU	0.8505	0.86	-0.1391 \pm 0.3941	0.000 \pm 0.616	0.198 \pm 0.087
78	LEU				-0.174 \pm 0.034	0.172 \pm 0.135
79	GLU	0.8028	0.8093	-0.0725 \pm 0.3512	-0.274 \pm 0.011	-0.052 \pm 0.062
80	LYS	0.8451	0.8256	0.2515 \pm 0.3554	0.000 \pm 0.616	0.099 \pm 0.192
81	SER	0.8412	0.8294	0.152 \pm 0.3548	-1.700 \pm 0.315	-0.039 \pm 0.065
82	GLY					
83	GLU	0.8173	0.8029	0.1625 \pm 0.3659	1.283 \pm 0.492	0.122 \pm 0.067
84	THR	0.8072	0.8092	-0.0223 \pm 0.3545	0.757 \pm 0.017	0.099 \pm 0.064
85	GLY				0.000 \pm 0.616	0.189 \pm 0.055
86	ILE	0.8817	0.8581	0.3814 \pm 0.401	-1.380 \pm 0.323	0.382 \pm 0.132
87	GLU	0.8241	0.8033	0.2388 \pm 0.3717	0.000 \pm 0.616	-0.073 \pm 0.072
88	GLU	0.8338	0.8187	0.1843 \pm 0.4058	0.000 \pm 0.616	0.002 \pm 0.094
89	GLY				3.715 \pm 0.332	-0.200 \pm 0.110
90	CYS	0.8341	0.8474	-0.1777 \pm 0.3809	1.642 \pm 0.323	0.087 \pm 0.207
91	LEU	0.9471	1	-0.5847 \pm 0.4232	0.948 \pm 0.326	-0.335 \pm 0.179
92	SER	0.9631	0.9665	0 \pm 0.3669	2.329 \pm 0.372	-0.179 \pm 0.126
93	ILE	0.9285	0.9436	-0.4854 \pm 0.3861	-2.372 \pm 0.412	
94	PRO					
95	GLU				0.000 \pm 0.616	0.359 \pm 0.073
96	GLN					
97	ARG	0.7682	0.7119	0.4821 \pm 0.4551		0.055 \pm 0.104
98	ALA				1.206 \pm 0.078	
99	LEU					-0.068 \pm 0.060
100	VAL	0.8653	0.8596	0.0878 \pm 0.3755	-0.227 \pm 0.016	-0.123 \pm 0.086
101	PRO					
102	ARG	0.7986	0.7863	0.129 \pm 0.3794	0.125 \pm 0.067	0.021 \pm 0.134
103	ALA				-0.007 \pm 0.170	
104	GLU	0.8615	0.8708	-0.1457 \pm 0.3598	0.066 \pm 0.086	-0.087 \pm 0.076
105	LYS	0.862	0.8528	0.1369 \pm 0.3666	0.000 \pm 0.616	0.044 \pm 0.180
106	VAL	0.8463	0.7856	0.7116 \pm 0.4529	-2.296 \pm 0.409	0.228 \pm 0.075
107	LYS	0.8265	0.7614	0.6884 \pm 0.486	-1.127 \pm 0.582	0.215 \pm 0.253
108	ILE	0.8725	0.8778	-0.0896 \pm 0.3742	-2.086 \pm 0.419	0.353 \pm 0.100
109	ARG	0.8718	0.8831	-0.1918 \pm 0.3628	0.000 \pm 0.616	0.367 \pm 0.115
110	ALA	0.8564	0.8541	0.0329 \pm 0.391	-1.464 \pm 0.424	0.156 \pm 0.075
111	LEU	0.8403	0.8649	-0.3518 \pm 0.3863	-2.257 \pm 0.408	0.155 \pm 0.085
112	ASP	0.8532	0.8518	0.0199 \pm 0.3511	-2.159 \pm 0.442	-0.103 \pm 0.094
113	ARG	0.8695	0.8619	0.1186 \pm 0.362		

Residue		S ² PDF +actinonin	S ² PDF	ΔS_{conf} \pm $\delta \Delta S_{\text{conf}}$	$\Delta \Delta G_{\text{HD}}$ \pm $\delta \Delta \Delta G_{\text{HD}}$	ΔrDC \pm $\delta \Delta rDC$
114	ASP	0.8604	0.8802	-0.3203 \pm 0.3749		
115	GLY	0.8719	0.8761	-0.0703 \pm 0.4135	-0.966 \pm 0.316	-0.155 \pm 0.129
116	LYS				0.344 \pm 0.099	
117	PRO					
118	PHE	0.8724	0.8735	-0.0182 \pm 0.3574	-1.868 \pm 0.382	-0.073 \pm 0.092
119	GLU	0.8223	0.8281	-0.0712 \pm 0.3455	0.000 \pm 0.616	0.116 \pm 0.086
120	LEU	0.8387	0.8389	-0.0031 \pm 0.3876	-1.840 \pm 0.390	0.238 \pm 0.085
121	GLU				0.000 \pm 0.616	0.285 \pm 0.077
122	ALA	0.8203	0.8261	-0.0704 \pm 0.398		
123	ASP	0.7811	0.7862	-0.0521 \pm 0.3636	0.000 \pm 0.616	0.118 \pm 0.060
124	GLY	0.7776	0.7518	0.2407 \pm 0.4056	0.000 \pm 0.616	0.007 \pm 0.067
125	LEU	0.9366	0.913	0.6452 \pm 0.5026	0.000 \pm 0.616	-0.010 \pm 0.124
126	LEU					-0.210 \pm 0.081
127	ALA	0.8743	0.8789	-0.0779 \pm 0.3584	0.000 \pm 0.616	0.111 \pm 0.055
128	ILE	0.8791	0.8692	0.164 \pm 0.3712	0.000 \pm 0.616	0.307 \pm 0.080
129	CYS	0.9029	0.9154	-0.2816 \pm 0.346	0.000 \pm 0.616	0.571 \pm 0.124
130	ILE	0.8964	0.8919	0.0877 \pm 0.3546	0.000 \pm 0.616	0.285 \pm 0.089
131	GLN					
132	HIS					
133	GLU	0.9549	0.9458	0.6342 \pm 0.4036	0.000 \pm 0.616	0.444 \pm 0.110
134	MET	0.9005	0.9365	-0.9206 \pm 0.3694	0.000 \pm 0.616	0.198 \pm 0.137
135	ASP					
136	HIS	0.9218	0.9193	0.0631 \pm 0.3942	0.000 \pm 0.616	0.169 \pm 0.118
137	LEU	0.911	0.9318	-0.5434 \pm 0.4033	0.000 \pm 0.616	0.066 \pm 0.067
138	VAL				0.000 \pm 0.616	0.072 \pm 0.079
139	GLY	0.9663	0.9622	0 \pm 0.4208	0.704 \pm 0.156	0.035 \pm 0.076
140	LYS					
141	LEU					
142	PHE					
143	MET	0.9078	0.8948	0.2723 \pm 0.3678		
144	ASP					
145	TYR	0.8887	0.865	0.4012 \pm 0.3753	0.000 \pm 0.616	-0.056 \pm 0.081
146	LEU	0.7829	0.7603	0.2166 \pm 0.485	0.000 \pm 0.616	-0.122 \pm 0.063
147	SER					

Table 3. Actinonin and Zn²⁺ input parameters for the program STC (11). (See Supplementary figure Figure 12)

```
# actinonin in 1G2A
RESIDUE ATOM BB2
THERMO -99  602.0  8.2  1.87 13.5
ATOM N  1.65 1 1
ATOM C5 1.87 0 1
ATOM C3 1.87 0 1
ATOM O4 1.40 1 0
ATOM N1 1.65 1 1
ATOM O2 1.40 1 0
ATOM C6 1.87 0 1
ATOM C12 1.76 0 1
ATOM O13 1.40 1 0
ATOM C7 1.76 0 0
ATOM C8 1.76 0 0
ATOM C9 1.87 0 0
ATOM C10 1.76 0 0
ATOM C11 1.76 0 0
ATOM N14 1.65 1 1
ATOM C15 1.87 0 1
ATOM C16 1.87 0 0
ATOM C18 1.87 0 0
ATOM C17 1.87 0 0
ATOM C19 1.87 0 1
ATOM O20 1.40 1 0
ATOM N21 1.65 1 1
ATOM C22 1.76 0 0
ATOM C23 1.76 0 0
ATOM C24 1.76 0 0
ATOM C25 1.76 0 0
ATOM C26 1.76 0 0
ATOM O27 1.40 1 0
#
RESIDUE ATOM ZN2
THERMO -99  0.0  0.0  0.00 0.00
ATOM O1 1.40 0 0
```

Table 4. Thermodynamic data for the PDF-actinonin interaction

Method	cal mol ⁻¹ K ⁻¹	kcal mol ⁻¹ at 310K
Structure-based (STC) ^a		
ΔS_{bind}	25	
ΔS_{sol}	43	
$\Delta S_{\text{t/r}}$	-8	
ΔS_{conf}	-9.3	
$T\Delta S_{\text{bind}}$		7.8
ΔC_p	-149	
K_D : 0.4 μM		
ΔH_{bind}		-1.23
ΔG_{bind}		-9.05
Calorimetry ^b		
ΔS_{bind}	27 \pm 4	
$T\Delta S_{\text{bind}}$		8.4 \pm 1.3
ΔH_{bind}		-1.644 \pm 0.012
ΔC_p	-180 \pm 10	
ΔG_{bind}		-9.8 \pm 1.3
K_A : 9.02 \pm 1.2 $\times 10^6 \text{ M}^{-1}$		
K_D : 111 \pm 15 nM		
NMR		
ΔS_{conf}		0 \pm 4

^a STC (11) calculations were performed with the temperature set to 310 K, and used chain A and ligand of 1G2A.pdb. The conformational entropy change of actinonin upon binding to PDF was estimated by assuming that all single bonds were free to adopt standard rotameric conformations in the free protein, but only one rotameric state in the complex. ^b Thermodynamic measurements were obtained by isothermal titration calorimetry (A. Simmons, BS thesis, 2007, Department of Biochemistry, The Ohio State University). Reported uncertainties are deviations from multiple measurements, except for ΔC_p , which is the standard error of the enthalpy data from best-fit values. Given: $\Delta S_{\text{bind}} = \Delta S_{\text{solv}} + \Delta S_{\text{rt}} + \Delta S_{\text{conf,prot}} + \Delta S_{\text{conf,actinonin}}$, and using the experimentally-determined value of $T\Delta S_{\text{bind}}$: $27 \pm 4 = 43 - 8 + \Delta S_{\text{conf,prot}} + \Delta S_{\text{conf,act}}$. This yields an estimate for the contribution from conformational entropy of $\Delta S_{\text{conf,prot}} + \Delta S_{\text{conf,act}} = 8 \pm 4 \text{ cal mol}^{-1} \text{ K}^{-1}$. Because the uncertainty in the estimated value is large relative to the precision of the measured parameters, it is risky to pursue this analysis further without additional data.

SUPPLEMENTARY FIGURES

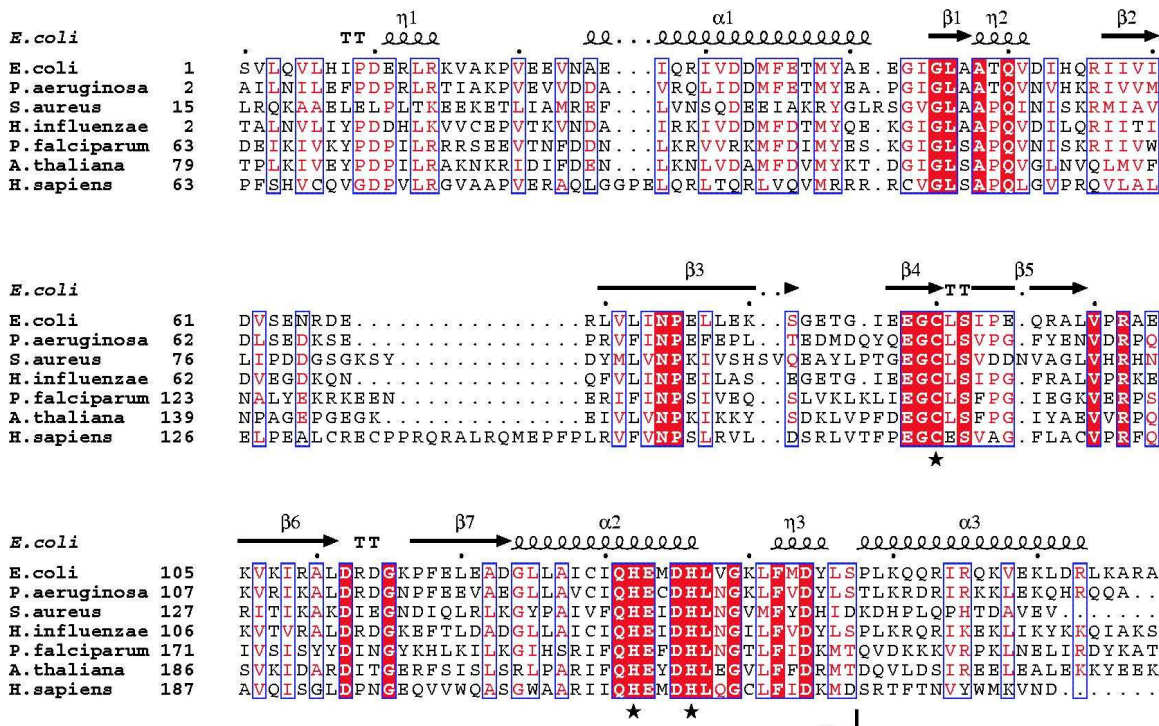


Figure 1. Sequence alignment of peptide deformylase enzymes from various organisms, including Bacteria and Eukarya. Alignments were generated using CLUSTALW (12), and the figure generated with ESPRIPT (13), using default settings for conservation. Invariant residues are indicated by white letters on a red background. Metal-binding ligands are indicated with a star. The site of truncation of the C-terminal helix (Ser147 in *E. coli* PDF) is indicated. Secondary structural features correspond to those in the PDB entry 1G2A.

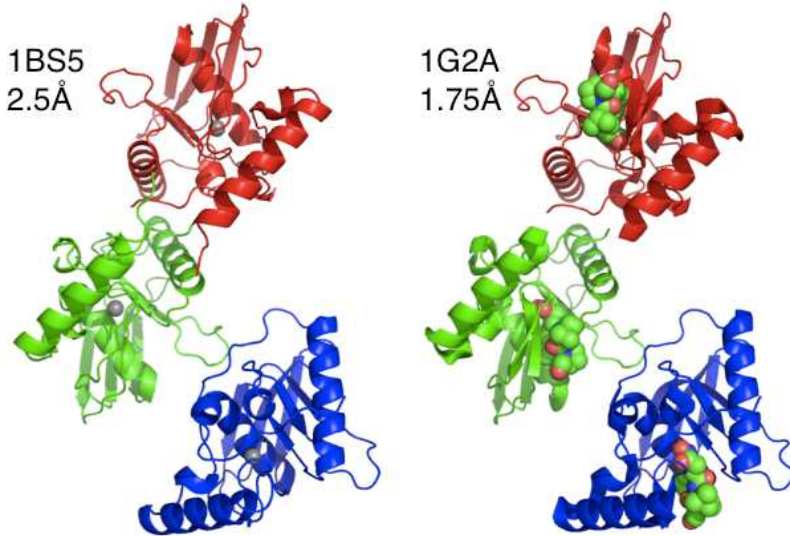


Figure 2. Ribbon diagrams for *E. coli* peptide deformylase (PDF) as observed in the crystal structures, 1BS5 (free) (14) and 1G2A (bound to actinonin) (15). The asymmetric unit consists of three molecules of PDF.

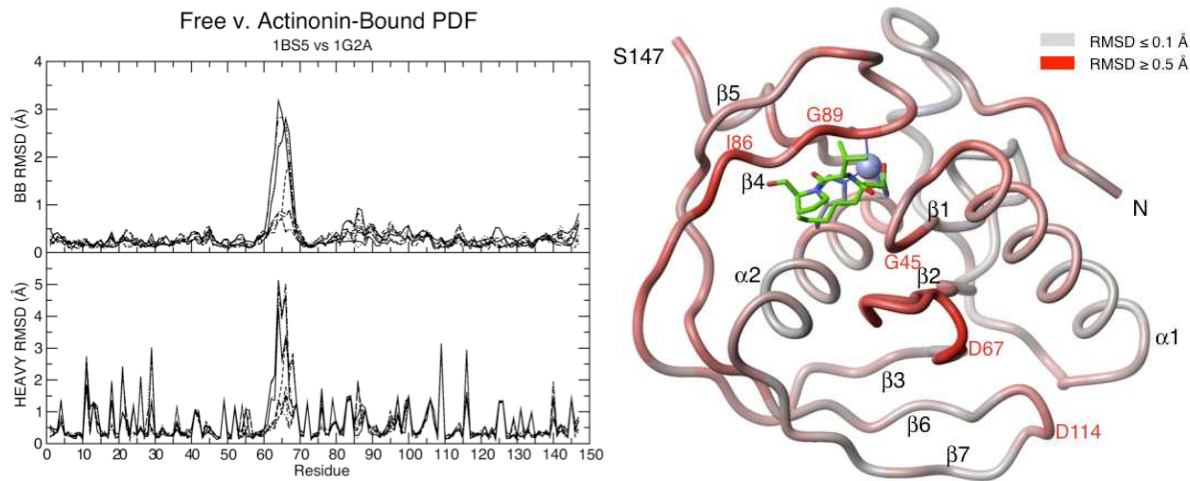


Figure 3. Differences in the coordinate positions between the molecules within the asymmetric unit, and between free and bound structures for, 1BS5 (free) and 1G2A (bound to actinonin). Top left, backbone atoms; bottom left sidechain heavy atoms. Calculated using MOLMOL (16). Right, backbone RMSDs mapped to a ribbon diagram of 1G2A.

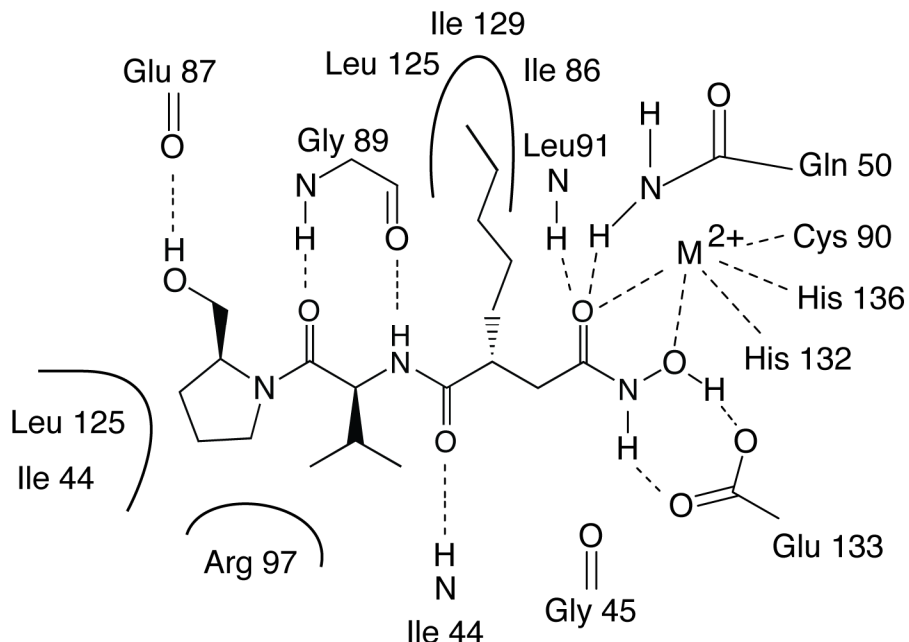


Figure 4. Contacts between actinonin and *E. coli* PDF, as observed in the crystal structure, 1G2A (15).

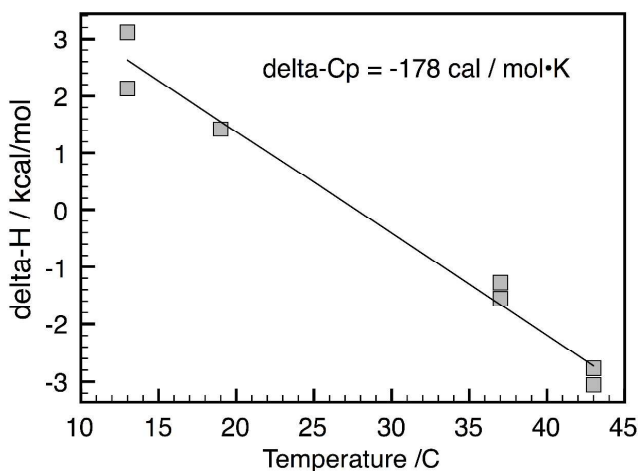


Figure 5. Effect of temperature on the enthalpy of PDF binding to actinonin, as measured by ITC. The slope of the line gives a best-fit value for ΔC_p ($= d\Delta H/dT$) of $-180 \pm 10 \text{ cal mol}^{-1} \text{ K}^{-1}$; the stated uncertainty is the standard error in the fit.

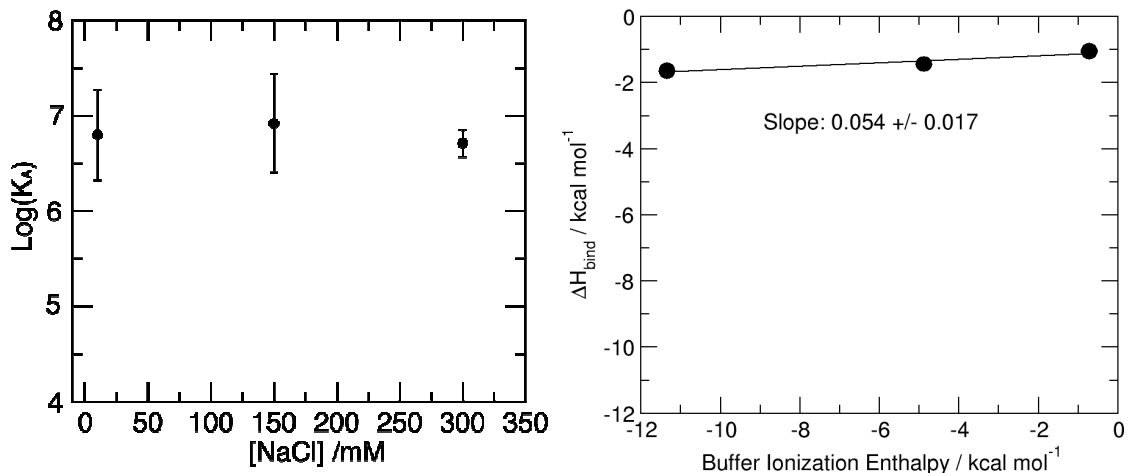


Figure 6. Effect of ionic strength (left) and buffer (right) on the affinity of PDF for actinonin, as measured by ITC. The absence of a significant effect of salt concentration on K_A indicates that ion linkage does not significantly contribute to the measured thermodynamic parameters. The slope of ΔH versus h_l gives the number of protons linked to the binding event; under these conditions, proton linkage does not appear to be a significant contribution to binding thermodynamics. Error bars are the standard fitting errors from individual ITC experiments; error in fitted enthalpy is within the size of the symbols.

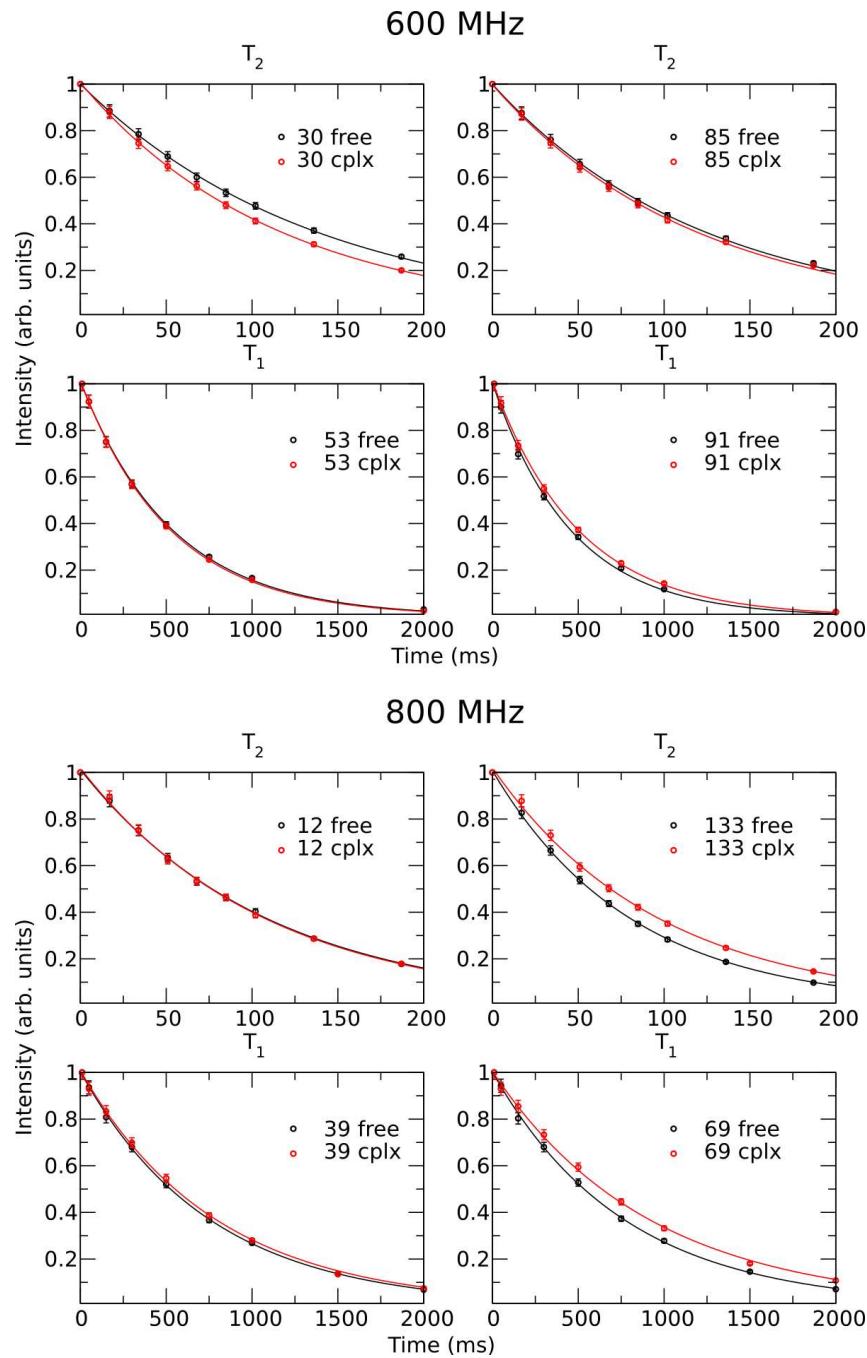


Figure 7. Fits of T_1 and T_2 decay curves for free and actinonin-bound PDF. Some residues experience a change in relaxation rates upon actinonin binding (e.g., Ala⁴⁷, Leu⁹¹ and Ser⁹²), while other residues do not (e.g., Glu⁸⁷, Cys⁹⁰ and Val¹⁰⁶). Data were recorded at (a) 600 MHz and (b) 800 MHz.

Backbone amide ^{15}N relaxation

PDF - Black PDF + actinonin - Red

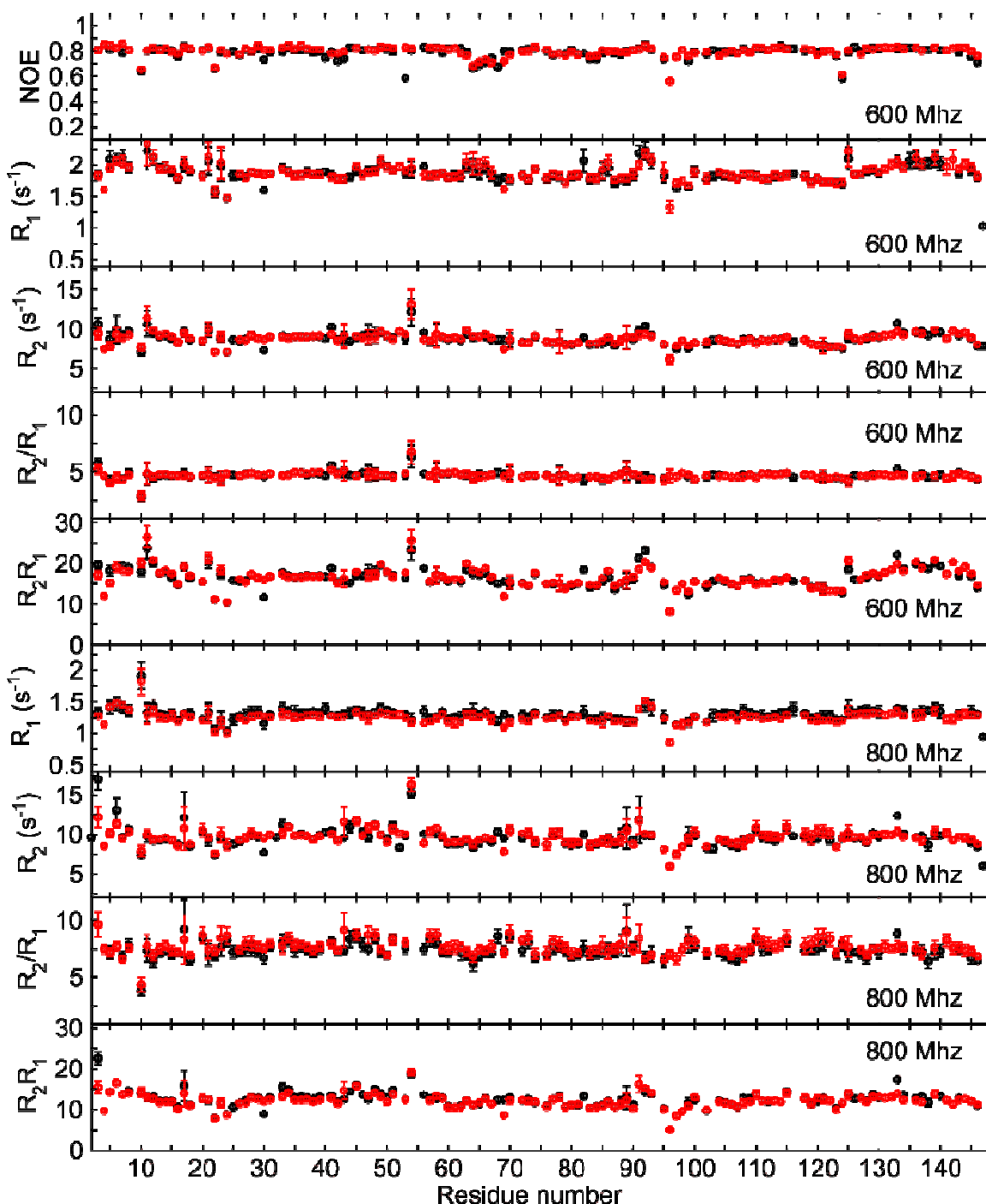


Figure 8. Backbone amide ^{15}N relaxation rate constants (R_1 , R_2 , $^{1\text{H}}\text{-}\{^{15}\text{N}\}$ NOE, R_2/R_1 and R_2R_1) for EcPDF in the absence (black) and presence (red) of actinonin. Top, 600 MHz, bottom, 800 MHz.

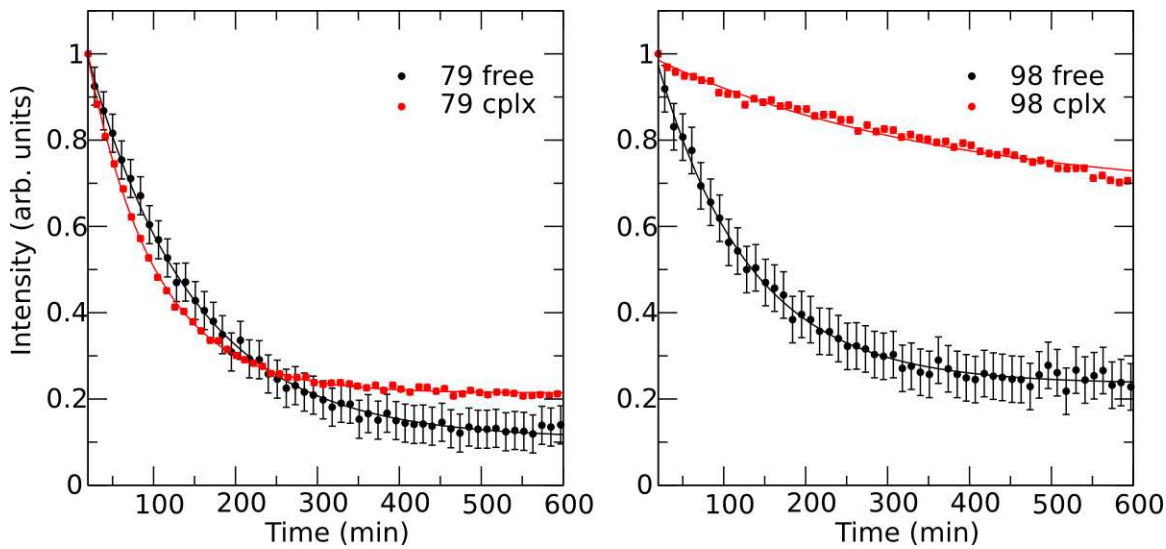


Figure 9. Hydrogen/Deuterium exchange curve fits for free and bound PDF. The curves are a plot of peak intensity from a series of ^{15}N HSQC spectra recorded in series. Times correspond to time after exchange into D_2O . Intensity data were fit to a two-parameter exponential of the form $I = \exp(-k_{\text{ex}}t) + C$, where the rate k_{ex} and endpoint C are the fitted parameters. The dead time of the experiments was 11 minutes.

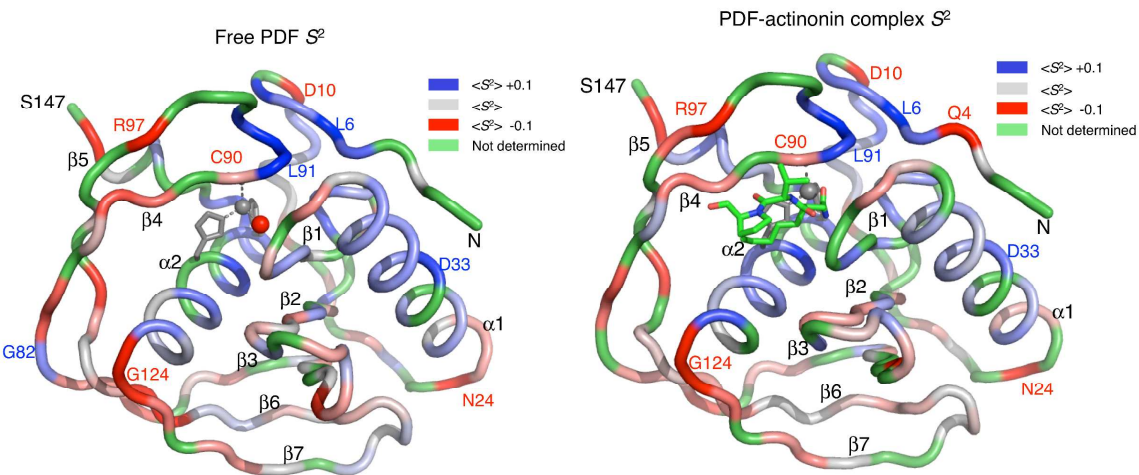
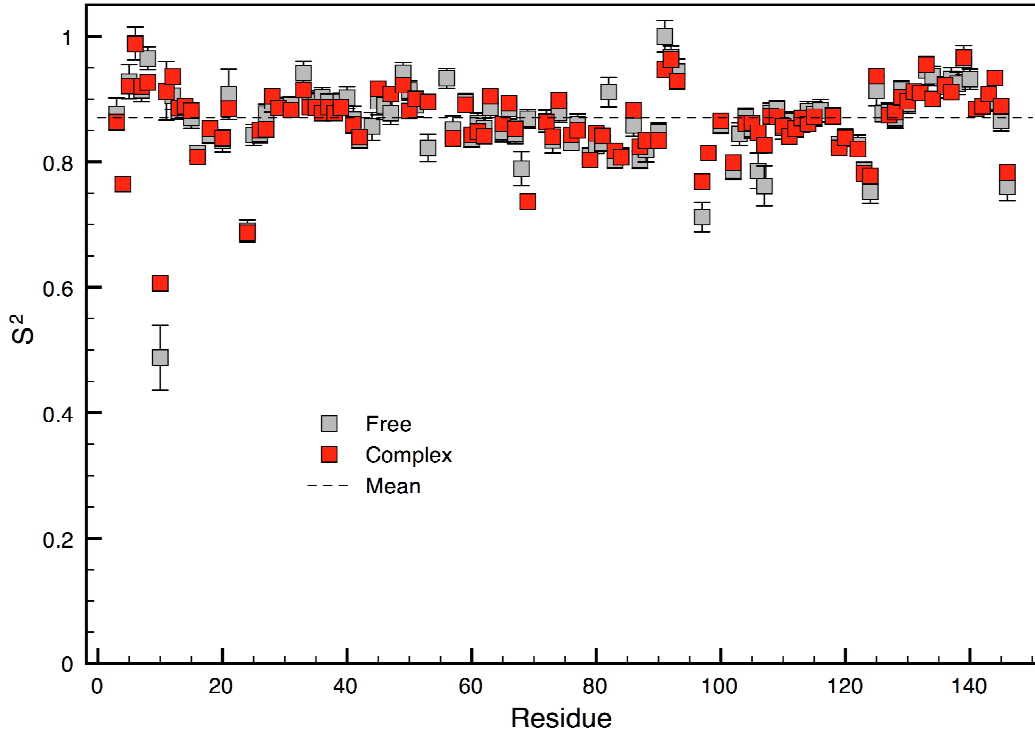
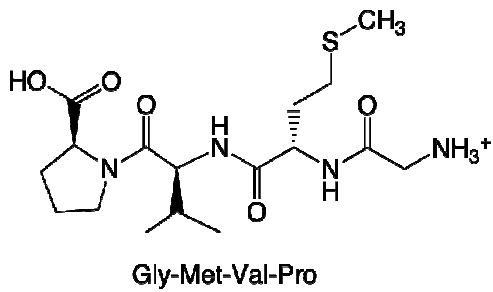


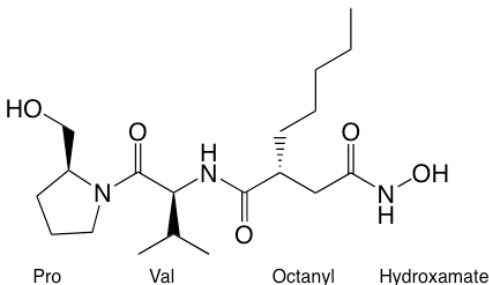
Figure 10. Model-Free order parameters (S^2) for free EcPDF (left) and the EcPDF-actinonin complex (right). Values are mapped with linear color ramps from grey (mean S^2 for free PDF, 0.87) to red for amides more dynamic than the mean ($S^2 \leq 0.77$) or blue for amides more rigid than the average ($S^2 \geq 0.97$). The 10% trimmed standard deviation in S^2 was 0.04 for free and 0.03 for the complex; 10% trimmed mean was 0.88 for the complex.



	Pro	Val	Met	Gly	Total
dS_{bu-ex}	0	0.12	4.55	0	4.7
dS_{Se-Xu}	0	1.29	0.58	0	1.87
dS_{BB}	1.4*	2.18	3.40	6.5	13.4

* Using $dS_{BB} = R \cdot \ln 2$ since cis/trans isomers are seen in NMR data of free actinonin

Figure 11. Peptide model for estimating structure-based ΔS_{conf} for actinonin. Based on data tables in (11, 17), and <http://www.bionmr.ualberta.ca/bds/software/stc/latest/files/amino.def.html>



	Pro	Val	Octanyl	Hydroxamate	Total
dS_{bu-ex}	0	0.12	8.07†	0	8.19
dS_{Se-Xu}	0	1.29	0.58	0	1.87
dS_{BB}	1.4*	2.18	3.40	6.5	13.5

* Our NMR spectra of free actinonin show two conformations for Pro, so reduction in states from 2 to 1 is 1.4 cal/mol·K. Using 18.2 as dS_{bu-ex} in STC yields 13 cal/mol·K or 4 kcal/mol at 310. † To Met value, added 2×1.76 for 2 extra rotatable bonds.

Figure 12. Estimating structure-based ΔS_{conf} for actinonin. Based on (11, 17), and data tables in <http://www.bionmr.ualberta.ca/bds/software/stc/latest/files/amino.def.html>

References

- (1) Spolar, R. S., and Record, M. T., Jr. (1994) Coupling of local folding to site-specific binding of proteins to DNA. *Science* 263, 777-784.
- (2) Lazaridis, T., Masunov, A., and Gandolfo, F. (2002) Proteins

- Contributions to the binding free energy of ligands to avidin and streptavidin. *Proteins* 47, 194-208.
- (3) Yu, Y. B., Privalov, P. L., and Hodges, R. S. (2001) Contribution of translational and rotational motions to molecular association in aqueous solution. *Biophys J* 81, 1632-1642.
 - (4) Luo, H., and Sharp, K. (2002) On the calculation of absolute macromolecular binding free energies. *Proc Natl Acad Sci U S A* 99, 10399-10404.
 - (5) Dunitz, J. D. (1994) The entropy cost of bound water in crystals and biomolecules. *Science* 264, 670.
 - (6) Byerly, D. W., PhD Dissertation (2002) *PhD Dissertation: Structure and dynamics of ligand binding to E. coli peptide deformylase*, Biochemistry Graduate Program, The Ohio State University, Columbus.
 - (7) Clements, J. M., Beckett, R. P., Brown, A., Catlin, G., Lobell, M., Palan, S., Thomas, W., Whittaker, M., Wood, S., Salama, S., Baker, P. J., Rodgers, H. F., Barynin, V., Rice, D. W., and Hunter, M. G. (2001) Antibiotic activity and characterization of BB-3497, a novel peptide deformylase inhibitor. *Antimicrob Agents Chemother* 45, 563-570.
 - (8) Freire, E. (1998) Statistical thermodynamic linkage between conformational and binding equilibria. *Adv Protein Chem* 51, 255-279.
 - (9) Baker, B. M., and Murphy, K. P. (1996) Evaluation of linked protonation effects in protein binding reactions using isothermal titration calorimetry. *Biophys J* 71, 2049-2055.
 - (10) Goldberg, R. N. K. N. L. R. M. (2002) Thermodynamic Quantities for the Ionization Reactions of Buffers. *J. Phys. Chem. Ref. Data* 31, 231-370.
 - (11) Lavigne, P., Bagu, J. R., Boyko, R., Willard, L., Holmes, C. F., and Sykes, B. D. (2000) Structure-based thermodynamic analysis of the dissociation of protein phosphatase-1 catalytic subunit and microcystin-LR docked complexes. *Protein Sci* 9, 252-264.
 - (12) Thompson, J. D., Higgins, D. G., and Gibson, T. J. (1994) CLUSTAL W: improving the sensitivity of progressive multiple sequence alignment through sequence weighting, position-specific gap penalties and weight matrix choice. *Nucleic Acids Res* 22, 4673-4680.
 - (13) Gouet, P., Courcelle, E., Stuart, D. I., and Metoz, F. (1999) ESPript: analysis of multiple sequence alignments in PostScript. *Bioinformatics* 15, 305-308.
 - (14) Becker, A., Schlichting, I., Kabsch, W., Schultz, S., and Wagner, A. F. (1998) Structure of peptide deformylase and identification of the substrate binding site. *J Biol Chem* 273, 11413-11416.
 - (15) Clements, J. M., Beckett, R. P., Brown, A., Catlin, G., Lobell, M., Palan, S., Thomas, W., Whittaker, M., Wood, S., Salama, S., Baker, P. J., Rodgers, H. F., Barynin, V., Rice, D. W., and Hunter, M. G. (2001) Antibiotic activity and characterization of BB-3497, a novel peptide deformylase inhibitor. *Antimicrob Agents Chemother* 45, 563-570.
 - (16) Koradi, R., Billeter, M., and Wuthrich, K. (1996) MOLMOL: a program for display and analysis of macromolecular structures. *J Mol Graph* 14, 51-55, 29-32.
 - (17) D'Aquino, J. A., Freire, E., and Amzel, L. M. (2000) Binding of small organic molecules to macromolecular targets: evaluation of conformational entropy changes. *Proteins Suppl* 4, 93-107.